

Received November 3, 2019, accepted November 10, 2019, date of publication November 14, 2019, date of current version November 27, 2019.

Digital Object Identifier 10.1109/ACCESS.2019.2953478

State of Charge Estimation for Lithium Battery Based on Adaptively Weighting Cubature Particle Filter

KAI ZHANG^{ID}, JIAN MA^{ID}, XUAN ZHAO^{ID}, DAYU ZHANG^{ID}, AND YILIN HE^{ID}

School of Automobile Engineering, Chang'an University, Xi'an 710064, China

Corresponding authors: Kai Zhang (zhangkai@chd.edu.cn) and Xuan Zhao (zhaoxuan@chd.edu.cn)

This work was supported in part by the National Key Research and Development Program of China under Grant 2017YFC0803904, in part by the China Postdoctoral Science Foundation under Grant 2018T111006 and Grant 2017M613034, in part by the Shaanxi Province Industrial Innovation Chain Project under Grant 2019ZDLGY15-01 and Grant 2019ZDLGY15-02, and in part by the Postdoctoral Science Foundation of Shaanxi Province under Grant 2017BSHEDZZ36.

ABSTRACT Accurate estimation of lithium battery state of charge is very important for ensuring the operation of battery management system, realizing the energy management strategy of electric vehicles, reducing mileage anxiety and promoting the sustainable development of electric vehicles. In this paper, several studies are carried out for state of charge estimation of lithium-ion battery: (1) Aiming at the problem of parameter identification of battery model, an optimal identification method of model parameters based on ant lion optimization algorithm is proposed. (2) An adaptive weighting Cubature particle filter (AWCPF) method is proposed for SOC estimation. The proposed AWCPF method is based on particle filter (PF) algorithm, while the Cubature Kalman filter (CKF) algorithm is utilized to generate the proposal distribution for PF algorithm, which can retrain the particles degradation problem in PF algorithm. To solve the problem that the CKF algorithm is sensitive to noise, comparing with fixed sigma point weights of the conventional CKF, the weights of sigma points are adaptively adjusted based on state and measurement residual vectors. Furthermore, the process noise and measurement noise are estimated iterative. In this paper, experimental verification of different initial values of SOC under various working conditions is carried out. The results show that the proposed AWCPF algorithm based SOC estimation method has high estimation accuracy, strong robustness, fast convergence speed, with the maximum SOC estimation error is less than 1%.

INDEX TERMS Adaptive weighting factors, cubature particle filter, lithium battery, state of charge.

I. INTRODUCTION

With the rapid development of electric vehicles, and as the core component of the energy storage system in electric vehicles, power batteries have become a bottleneck that restricts the development of electric vehicles [1], [2]. In recent years, lithium-ion power batteries have been extensively employed in various electric vehicles due to their high energy density, long service life and lack of memory effect. To satisfy the power demand of electric vehicles, a certain number of single cells are usually packed in series and parallel to overcome the disadvantages of single cells in terms of working voltage, energy density and capacity [3]–[6]. In addition, the instability and flammability of liquid electrolytes will

cause potential safety hazards for power batteries in abuse conditions, such as overcharge and overdischarge. Therefore, a battery management system (BMS) has an important role in improving the performance of power batteries and ensuring the safety and reliability operation of batteries. As one of the core functions of a BMS, accurate state of charge (SOC) estimation is helpful not only for improving the efficiency of energy management and the cycle life of power battery, but also for reducing the utilization cost and facilitating the development of electric vehicles [7]–[9]. However, the performance of power batteries substantially depends on their working environment and aging degree, which cannot be accurately controlled.

The SOC cannot be directly measured and has to be estimated based on several measured signals, such as voltage, current and temperature. Many SOC estimation methods

The associate editor coordinating the review of this manuscript and approving it for publication was Zhen Li.

have been proposed by researchers. The coulomb counting method is the most prevalent and simple method of SOC estimation; however, it has some shortcomings. As an open-loop calculation method, the coulomb counting method lacks a self-correction link. The uncertainty disturbance in practical application and the deviation of the initial SOC value will generate errors that gradually accumulate with the running time, which is adverse to the estimation accuracy [10]–[12]. Another commonly employed method is the data-driven method, which is an intelligent algorithm for identifying the relationship between the input and the output, including the neural network, support vector machine, and fuzzy inference system [13]–[16]. However, shortages exist in the data-driven method, such as the larger amount of data scales that are required for the training period, and the high computer cost due to the complicated structure of intelligent algorithms, which are not suitable for practical application. The third general SoC estimation method is based on the filter and battery model. The most commonly employed filter estimation algorithm is the Kalman filter algorithms, which is based on the state space equation and integrates the Ah counting method into the equations. The Extended Kalman filter (EKF) is one kind of Kalman filter algorithm that employs a nonlinear system and is based on the first-order Taylor expansion of traditional nonlinear functions. The EKF has a simple structure that is easily implemented. However, the EKF has several distinct shortcomings: (1) If the system has strong nonlinearity, the linearization process will introduce large truncation error; (2) When the nonlinear function is not differentiable, the EKF is not workable [17]–[20]. To overcome the limitations of the EKF, an unscented Kalman filter (UKF) is proposed. The UKF uses a series of sample points to approximate the mean and covariance of the posterior probability density function of the state vector. The UKF does not approximate the nonlinear function, nor does it need to approximate the Jacobian matrix. Compared with the EKF, the UKF has the advantages of simple implementation, high filtering accuracy and excellent convergence. However, the UKF requires precise prior knowledge of system noise, which is difficult to obtain in practice, since the application environment is always dynamic and uncertain. When the statistical characteristics of measurement noise are uncertain, the filtering accuracy will decrease or even diverge [21]–[24]. In our previous work [25], the knowledge of system noise is obtained by an improved ant lion algorithm, which demonstrate high accuracy and efficiency.

Unfortunately, the EKF and UKF algorithms require the system noise to be the Gaussian distribution. For non-Gaussian system noise, the algorithms are infeasible. Instead, the particle filter (PF), which is based on probability distribution theory, can handle any nonlinear model and arbitrary distribution of noise [26]–[28]. The application of PF for SOC estimation has been verified with satisfactory performance by many studies [29]–[31]. Reference [5] conducted a comprehensive analysis of the application of PF for

SOC estimation, they recommend PF as a promising method for SOC estimation.

However, the PF suffers several shortages, such as high computation burden and particle impoverishment. Some researchers applied an event-trigger strategy to reduce the computation cost. This strategy only transmits the observations that contain innovational information to the estimation center, which can substantially reduce the communication and computation burden. Various event-trigger strategies for KF or PF were proposed [32]–[37]. The event-trigger strategy is suitable for a smart grid system, which has a large amount of data to be transmitted. Another possible method of reducing the computation cost is the parallel processing, since each particle of PF can be separately processed. To overcome the shortages of particle impoverishment and model parameters perturbation that exist in the PF algorithm, UKF and PF are combined to form an unscented particle filter (UPF) algorithm, which has shown higher accuracy for SOC estimation [38], [39]. The cubature Kalman filter (CKF) has attracted extensive attention in the field of nonlinear filtering systems, which applies the third-order spherical-radial cubature criterion to approximate the probability density function. The filtering accuracy is better than that of the UKF. All weights of the sampling points are identical and positive; thus, its numerical stability is also higher than that of the UKF [40]–[42]. An inspired idea is to use the CKF to generate the proposal distribution for the PF and construct the cubature particle filter (CPF), which can prevent the impoverishment of a particle and is more precise than the UPF [41].

This paper presents an adaptive weighting cubature particle filter (AWCPF). Considering that the CPF is sensitive to noise, the statistics of system noise, prediction state, measurement vector and covariance are estimated by an adaptive weighting method. The weights of cubature points are adjusted based on the adaptively weighting estimation, which can restrain the interference of system noise to state estimation and improve the stability of algorithm.

The remainder of the paper is arranged as follows: Section 2 presents the battery model and the model parameters identification method. Section 3 describes the proposed adaptive weighting cubature particle filter algorithm. The experimental results are analyzed in section 4. Section 5 provides the conclusion and future work.

II. BATTERY MODEL AND MODEL PARAMETERS IDENTIFICATION

A. BATTERY MODEL

Establishing an accurate and concise model has an important influence on the accuracy and calculation speed of the SOC estimation. Based on the application characteristics of lithium-ion batteries in EVs, an equivalent circuit model with resistance and capacitance as the core components has more advantages in structure and accuracy than other battery models. Xin Lai et al. investigated eleven ECMs which include a different number of RC networks and the hysteresis

phenomenon of open circuit voltage (OCV). In consideration of the accuracy, stability, complexity and computation cost of SOC estimation, their results demonstrate that the first-order RC model is the best ECM for the LiNCM battery [43]. Therefore, this paper utilizes the first-order RC equivalent circuit model to perform follow-up research. The model consists of three parts: the voltage source, which is the open-circuit voltage of power battery, represented by the OCV; the ohmic internal resistance, which represents the resistance of the battery electrode material, electrolyte, separator and contact resistance of the components, which is represented by R_i . The RC network, which describes the dynamic characteristics of a battery, including the polarization characteristics and diffusion effects, can be described by the polarization resistance R_d and the polarization capacitance C_d . The structure of the ECM is shown in Fig. 1.

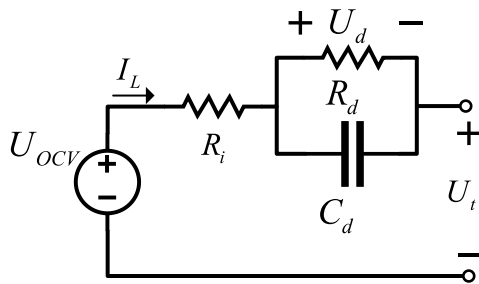


FIGURE 1. Structure of ECM.

where U_{OCV} is the open-circuit voltage, U_t is the terminal voltage, and U_d is the polarization voltage. I_L is the load current (which is set to positive for discharge and negative for charge). The electrical characteristics of the model can be expressed as

$$\begin{cases} \dot{U}_d = -\frac{1}{C_d R_d} U_d + \frac{1}{C_d} I_L \\ U_t = U_{ocv} - U_d - I_L R_i \end{cases} \quad (1)$$

where the terminal voltage U_t and the load current I_L are directly measured by high precision sensors. The polarization voltage U_d is an intermediate variable. The open circuit voltage U_{OCV} is the function of the SOC. In this paper, the low current (C/20) method is employed to obtain the relationship between OCV and SOC, and the OCV-SOC curve can be fitted by the following equation

$$U_{OCV}(z) = K_0 + K_1 z + K_2 z^2 + K_3 z^3 + K_4/z + K_5 \ln(z) + K_6 \ln(1-z) \quad (2)$$

where $K_i (i = 0, 1, \dots, 6)$ are multinomial coefficients that are fitted based on experimental data by least square method, and z denotes the state of charge (SOC) of battery.

In (1), the ohmic internal resistance R_i , polarization resistance R_d and polarization capacitance C_d are battery parameters that have to be identified by an optimization algorithm based on measured data. Details of parameter optimization algorithm are presented in the following section.

B. PARAMETER IDENTIFICATION METHOD

To apply the optimization algorithm for parameter identification, the battery model is discretized and rewritten as

$$\begin{cases} U_{d,k+1} = e^{-\frac{\Delta t}{\tau}} U_{d,k} + (1 - e^{-\frac{\Delta t}{\tau}}) R_d I_{L,k} \\ U_{t,k} = U_{OCV,k} - U_{d,k} - I_{L,k} R_i \end{cases} \quad (3)$$

where Δt is the sample interval and assumed be 1s in this paper; τ is the time constant which equals $\tau = R_d C_d$; and k is an integer variable that denotes the discrete index.

The model parameters, including R_i , R_d , and C_d , are identified by the improved ant lion optimization (IALO) algorithm which is a naturally inspired heuristic optimization algorithm that imitates the predatory behavior of an ant lion. The initial population of the IALO algorithm is $X = [R_i, R_d, C_d]$. The objective function is defined as:

$$f_{para} = \sum_{h=0}^N (U_{t,h} - U_{est,h})^2 \quad (4)$$

where N is the time length of the experiment data, $U_{t,h}$ denotes the measured terminal voltage at the h th sample time, and $U_{est,h}$ is the estimated terminal voltage at the h th sample time calculated by the corresponding individual (battery model parameters). The maximum iteration of the IALO is set to 500, and the iteration stops when the fitness of an elite individual does not change in 10 continuous iterations. By searching the solution space with random walk and comparing the fitness of individuals, the IALO algorithm can determine the optimal value of the battery model parameters. Readers can refer to [25] for details of the IALO algorithm.

III. PROPOSED SOC ESTIMATION METHODOLOGY

A. STATE OF CHARGE DEFINITION

State of charge is usually defined as the ratio of the remaining available capacity to the rated capacity of a battery. The discrete definition of SoC is expressed as:

$$z_k = z_{k-1} - \eta I_{L,k} \Delta t / C_n \quad (5)$$

where z_k is the SOC at the k th sampling time, C_n is the rated capacity; and η is the coulomb efficiency, which is related to the current rate, battery chemistry, and temperature. For simplicity, the coulomb efficiency is set to $\eta = 1$.

B. ADAPTIVE WEIGHTING CUBATURE PARTICLE FILTER

The accuracy and convergence speed of the particle filter (PF) algorithm is superior to other stochastic optimization algorithms [30]. However, a particle degradation problem exists in the PF algorithm, which can affect the performance of the PF method. This problem is caused by the difficulty of finding the optimal proposal distribution $q(x_k | x_{0:k-1}, y_k)$. A substituted option is to generate the approximate optimum proposal distribution from the latest information of x_{k-1} and y_k by some different methods. The high performance of the cubature Kalman filter has been verified for generating the proposal distribution for PF [41]. Therefore, this paper incorporates the CKF to generate approximate optimum proposal distribution for the PF to avoid the degradation of particles.

To apply the CKF algorithm, the nonlinear battery model has to be rewritten in the form of state space and is described as

$$\begin{cases} x_k = \begin{bmatrix} U_{d,k} \\ z_k \end{bmatrix} = f(x_k, u_k) + \omega_k \\ y_k = U_{t,k} = h(x_k, u_k) + v_k \\ f(x_k, u_k) = \begin{bmatrix} e^{-\Delta t/\tau} U_{d,k-1} + (1 - e^{-\Delta t/\tau}) R_d I_{L,k} \\ z_{k-1} - \eta I_{L,k} \Delta t / C_n \end{bmatrix} \\ h(x_k, u_k) = U_{oc,k} - U_{d,k} - R_i I_{L,k} \\ \omega_k \sim N(0, Q_k), \quad v_k \sim N(0, R_k) \end{cases} \quad (6)$$

where $x_k = [U_{d,k} \ z_k]^T$ is the state vector, and the system input vector u_k is the load current $I_{L,k}$. The output vector y_k is the terminal voltage $U_{t,k}$, and ω_k and v_k represent the mean of the process noise and the mean of the measurement noise, respectively, and their covariance matrixes are Q_k and R_k , respectively.

The basic steps of the CKF are expressed as follows:

1. Initialization of state and covariance

$$\begin{aligned} \hat{x}_0 &= E[x_0] \\ P_0 &= \text{cov}(x_0, x_0^T) = E[(x_0 - \hat{x}_0)(x_0 - \hat{x}_0)^T] \end{aligned} \quad (7)$$

2. Calculate the current state cubature points

$$\begin{aligned} P_{k-1|k-1} &= S_{k-1|k-1} S_{k-1|k-1}^T \\ \hat{x}_{i,k-1|k-1} &= S_{k-1|k-1} \xi_i + \bar{x}_{k-1|k-1}, \quad i = 1, \dots, 2n \end{aligned} \quad (8)$$

where ξ_i represents the cubature points and the corresponding weights are ω_i , which are defined as:

$$\xi_i = \sqrt{m/2} [1]_i \quad \omega_i = 1/m, \quad i = 1, \dots, m, m = 2n \quad (9)$$

where m is the number of cubature points, which is usually set to twice the dimension of the state vector n . $[1] \in R_{n \times m}$ is predefined constant matrix:

$$[1] = \left\{ \begin{bmatrix} 1 \\ 0 \\ \vdots \\ 0 \end{bmatrix}, \begin{bmatrix} 0 \\ 1 \\ \vdots \\ 0 \end{bmatrix}, \dots, \begin{bmatrix} 0 \\ 0 \\ \vdots \\ 1 \end{bmatrix}, \begin{bmatrix} -1 \\ 0 \\ \vdots \\ 0 \end{bmatrix}, \begin{bmatrix} 0 \\ -1 \\ \vdots \\ 0 \end{bmatrix}, \dots, \begin{bmatrix} 0 \\ 0 \\ \vdots \\ -1 \end{bmatrix} \right\}_{n \times m}$$

3. State prediction

Propagate the cubature points

$$\hat{x}_{i,k|k-1} = f(\hat{x}_{i,k-1|k-1}, u_{k-1}), \quad i = 1, \dots, 2n \quad (10)$$

State and error covariance prediction

$$\bar{x}_{k|k-1} = (1/m) \sum_{i=1}^m \hat{x}_{i,k|k-1}$$

$$\begin{aligned} P_{k|k-1} &= (1/m) \sum_{i=1}^m (\hat{x}_{i,k|k-1} - \bar{x}_{k|k-1}) (\hat{x}_{i,k|k-1} - \bar{x}_{k|k-1})^T \\ &\quad + Q_{k-1} \end{aligned} \quad (11)$$

4. Recalculate the cubature points

$$\begin{aligned} P_{k|k-1} &= S_{k|k-1} S_{k|k-1}^T \\ \hat{X}_{i,k|k-1} &= S_{k|k-1} \xi_i + \bar{x}_{k|k-1}, \quad i = 1, \dots, 2n \end{aligned} \quad (12)$$

5. Propagate the cubature points and predict the measurement

$$\begin{aligned} \hat{y}_{i,k|k-1} &= h(\hat{X}_{i,k|k-1}, u_k), \quad i = 1, \dots, 2n \\ \bar{y}_{k|k-1} &= (1/m) \sum_{i=1}^m \hat{y}_{i,k|k-1} \end{aligned} \quad (13)$$

6. Estimate the innovations covariance matrix and the cross-covariance matrix

$$\begin{aligned} P_{yy,k|k-1} &= (1/m) \sum_{i=1}^m (\hat{y}_{i,k|k-1} - \bar{y}_{k|k-1}) (\hat{y}_{i,k|k-1} - \bar{y}_{k|k-1})^T + R_k \\ P_{xy,k|k-1} &= (1/m) \sum_{i=1}^m (\hat{y}_{i,k|k-1} - \bar{y}_{k|k-1}) (\hat{X}_{i,k|k-1} - \bar{x}_{k|k-1})^T \end{aligned} \quad (14)$$

7. Calculate the Kalman gain and update the state and error covariance

$$\begin{aligned} K_k &= P_{xy,k|k-1} (P_{yy,k|k-1})^{-1} \\ \hat{x}_{k|k} &= \bar{x}_{k|k-1} + K_k (y_k - \bar{y}_{k|k-1}) \\ P_{k|k} &= P_{k|k-1} - K_k P_{yy,k|k-1} K_k^T \end{aligned} \quad (15)$$

In the process of practical application, the statistical characteristics of the process noise and measurement noise of the system are highly random and vulnerable to external environmental factors. Therefore, to further improve the estimation accuracy, a weighting factor method for the adaptive adjustment of system noise and measurement noise is proposed.

The residual vectors Δx and Δy are defined as

$$\begin{aligned} \Delta x_j &= \hat{x}_{j,k|k} - \hat{x}_{j,k|k-1} \quad (j = 1, 2, \dots, 2n) \\ \Delta y_j &= y_k - \hat{y}_{j,k|k-1} \end{aligned} \quad (16)$$

When the statistical characteristics of the process noise change, the contribution of $\hat{x}_{i,k|k-1}$ to the state estimation decreases, which cause a deviation of the state estimation and increase of the residual vector of the state estimation. Similarly, the variation in the measurement noise will affect the residual vector of the measurement estimation, which cause a deviation of the predicted values. Let

$$\omega_j = \|\Delta x_j\| \cdot \|\Delta y_j\| \quad (j = 1, 2, \dots, 2n) \quad (17)$$

where $\|\Delta x_j\| = \sqrt{\Delta x_j^T \Delta x_j}$, $\|\Delta y_j\| = \sqrt{\Delta y_j^T \Delta y_j}$. Normalizing ω_j , the adaptive weight factors are calculated by

$$\lambda_j = \omega_j / \sum_{j=1}^{2n} \omega_j, \quad (j = 1, 2, \dots, 2n) \quad (18)$$

The weighted estimation of the noise statistical characteristics enables adaptive adjustment of the weights of the cubature points to improve the performance of the state and measurement prediction, which can also restrain the influence of system noise on state estimation [44], [45]. Based on this analysis, the adaptive weighting cubature Kalman filter (AWCKF) is developed, which is described as follows:

1. Initialization of state and covariance

$$\begin{aligned} \hat{x}_0 &= E[x_0] \\ P_0 &= \text{cov}(x_0, x_0^T) = E[(x_0 - \hat{x}_0)(x_0 - \hat{x}_0)^T] \end{aligned} \quad (19)$$

2. Calculate the current state cubature points

$$\begin{aligned} P_{k-1|k-1} &= S_{k-1|k-1} S_{k-1|k-1}^T \\ \hat{x}_{i,k-1|k-1} &= S_{k-1|k-1} \xi_i + \hat{x}_{k-1|k-1}, \quad i = 1, \dots, 2n \end{aligned} \quad (20)$$

3. State prediction

Propagate the cubature points

$$\hat{x}_{i,k|k-1} = f(\hat{x}_{i,k-1|k-1}, u_{k-1}), \quad i = 1, \dots, 2n \quad (21)$$

State and error covariance prediction

$$\begin{aligned} \bar{x}_{k|k-1} &= \sum_{i=1}^m \lambda_i \hat{x}_{i,k|k-1} + \hat{q}_{k-1} \\ P_{k|k-1} &= \sum_{i=1}^m \lambda_i (\hat{x}_{i,k|k-1} - \bar{x}_{k|k-1})(\hat{x}_{i,k|k-1} - \bar{x}_{k|k-1})^T \\ &\quad + \hat{Q}_{k-1} \end{aligned} \quad (22)$$

4. Recalculate the cubature points

$$\begin{aligned} P_{k|k-1} &= S_{k|k-1} S_{k|k-1}^T \\ \hat{X}_{i,k|k-1} &= S_{k|k-1} \xi_i + \bar{x}_{k|k-1}, \quad i = 1, \dots, 2n \end{aligned} \quad (23)$$

5. Propagate the cubature points and predict measurement

$$\begin{aligned} \hat{y}_{i,k|k-1} &= h(\hat{X}_{i,k|k-1}, u_k), \quad i = 1, \dots, 2n \\ \bar{y}_{k|k-1} &= \sum_{i=1}^m \lambda_i \hat{y}_{i,k|k-1} + \hat{r}_{k-1} \end{aligned} \quad (24)$$

6. Estimate the innovations covariance matrix and the cross-covariance matrix

$$\begin{aligned} P_{yy,k|k-1} &= \sum_{i=1}^m \lambda_i (\hat{y}_{i,k|k-1} - \bar{y}_{k|k-1})(\hat{y}_{i,k|k-1} - \bar{y}_{k|k-1})^T + \hat{R}_{k-1} \\ P_{xy,k|k-1} &= \sum_{i=1}^m \lambda_i (\hat{y}_{i,k|k-1} - \bar{y}_{k|k-1})(\hat{X}_{i,k|k-1} - \bar{x}_{k|k-1})^T \end{aligned} \quad (25)$$

7. Calculate the Kalman gain and update the state and error covariance

$$K_k = P_{xy,k|k-1}(P_{yy,k|k-1})^{-1}$$

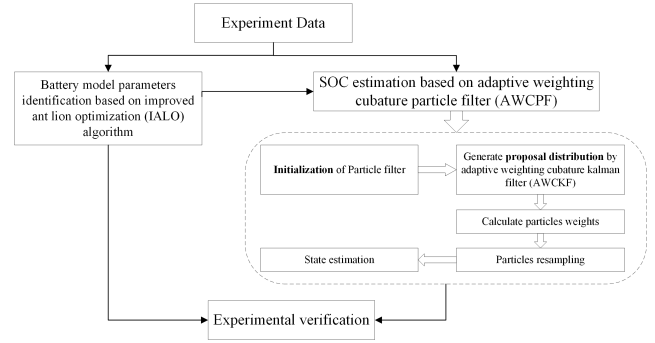


FIGURE 2. Flowchart of the proposed method for SOC estimation.

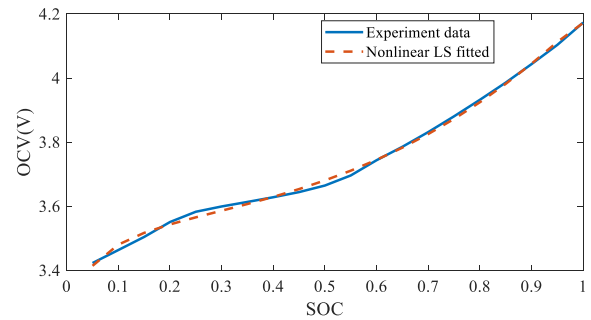


FIGURE 3. Results of OCV-SOC mapping test.

$$\begin{aligned} \hat{x}_{k|k} &= \bar{x}_{k|k-1} + K_k(y_k - \bar{y}_{k|k-1}) \\ P_{k|k} &= P_{k|k-1} - K_k P_{yy,k|k-1} K_k^T \end{aligned} \quad (26)$$

8. Estimate the statistics of noise

$$\begin{aligned} \hat{q}_k &= \frac{1}{k} \left[(k-1)\hat{q}_{k-1} + \hat{x}_{k|k} - \sum_{i=1}^{2n} \lambda_i \hat{x}_{i,k|k-1} \right] \\ \hat{Q}_k &= \frac{1}{k} \left[(k-1)\hat{Q}_{k-1} + \text{diag}[\hat{x}_{k|k} \hat{x}_{k|k}^T + P_{k|k} - \hat{q}_k \hat{q}_k^T] \right. \\ &\quad \left. - \sum_{i=1}^m \lambda_i \hat{x}_{i,k|k-1} \hat{x}_{i,k|k}^T - \sum_{i=1}^m \lambda_i \hat{x}_{i,k|k-1} \hat{x}_{i,k|k-1}^T \right. \\ &\quad \left. + \sum_{i=1}^m \lambda_i \hat{x}_{i,k|k-1} \hat{x}_{i,k|k-1}^T \right] \\ \hat{r}_k &= \frac{1}{k} \left[(k-1)\hat{r}_{k-1} + y_k - \sum_{i=1}^{2n} \lambda_i \hat{y}_{i,k|k-1} \right] \\ \hat{R}_k &= \frac{1}{k} \left[(k-1)\hat{R}_{k-1} + \text{diag}[y_k y_k^T - \hat{r}_k \hat{r}_k^T - \sum_{i=1}^m \lambda_i h(\hat{x}_{i,k|k}) y_k^T] \right. \\ &\quad \left. - y_k^T \sum_{i=1}^m \lambda_i h(\hat{x}_{i,k|k})^T + \sum_{i=1}^m \lambda_i h(\hat{x}_{i,k|k}) h(\hat{x}_{i,k|k})^T \right] \end{aligned} \quad (27)$$

The proposed SOC estimation method is based on PF, which utilizes the information estimated by the AWCKF to approximate the proposal distribution $q(x_k | x_{0:k-1}, y_k)$. The steps of the proposed adaptive weighting cubature particle filter (AWCPF) based SOC estimation method are expressed as follow:

1. Parameter initialization of $x_0, P_{0|0}, Q_0, R_0$, and ξ . Set the particle size to N , and the sample particles to $x_0^i, i =$

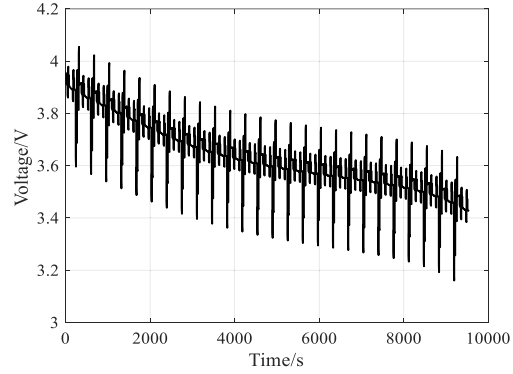
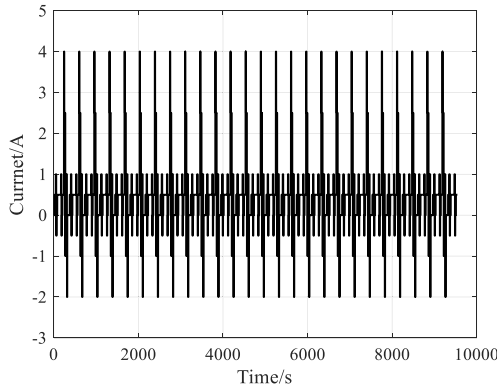


FIGURE 4. The current and voltage profiles under DST test condition.

- 1, \dots, N from x_0 and $P_{0|0}$. The initial weight of each particle is $w_0^i = 1/N$.
2. Calculate the state estimation $\hat{x}_{k|k}^i$ and the covariance $\hat{P}_{k|k}^i$ of every particle via AWCKF.
3. Update particles by sampling from the proposal distribution

$$\hat{x}_k^i \sim q\left(x_k^i \mid x_{0:k-1}^i, y_k\right) = N\left(\hat{x}_{k|k}^i, \hat{P}_{k|k}^i\right) \quad (28)$$

4. Calculate the weights of particles

$$w_k^i \propto \frac{p(y_k \mid x_k^i) p(x_k^i \mid x_{k-1}^i)}{q(x_k^i \mid x_{0:k-1}^i, y_k)} \quad (29)$$

$$\begin{aligned} & p(y_k \mid x_k^i) \\ &= \frac{1}{\sqrt{2\pi R_k}} \exp\left(-\frac{(y_k - h(\hat{x}_{k|k}^i, u_k))(y_k - h(\hat{x}_{k|k}^i, u_k))^T}{2R_k}\right) \\ & p(x_k^i \mid x_{k-1}^i) \\ &= \frac{1}{\sqrt{2\pi Q_{k-1}}} \\ & \quad \times \exp\left(-\frac{(\hat{x}_k^i - f(x_{k-1}^i, u_{k-1}))(\hat{x}_k^i - f(x_{k-1}^i, u_{k-1}))^T}{2Q_{k-1}}\right) \\ & q(x_k^i \mid x_{0:k-1}^i, y_k) \\ &= \frac{1}{\sqrt{2\pi \hat{P}_{k|k}^i}} \exp\left(-\frac{(\hat{x}_k^i - \hat{x}_{k|k}^i)(\hat{x}_k^i - \hat{x}_{k|k}^i)^T}{2\hat{P}_{k|k}^i}\right) \end{aligned} \quad (30)$$

5. Normalize the weights and resample the particle sets \hat{x}_k^i and $\hat{P}_{k|k}^i$ based on the weight values via a residual resampling method and obtain the new particle sets x_k^i and the responding covariance $P_{k|k}^i$.
6. The state estimation is calculated by

$$x_k = E(x_k^i) \quad (31)$$

where x_k is the state estimation at the k th sampling time via the adaptive weighting cubature particle filter (AWCPF) algorithm.

TABLE 1. Basic information of test cells.

Nominal voltage (V)	Nominal capacity (Ah)	Upper cut-off voltage (V)	Lower cut-off voltage (V)
3.6	2.0	4.2	2.5

TABLE 2. The fitted parameters of the OCV-SOC function.

K_0	K_1	K_2	K_3	K_4	K_5	K_6
3.7462	-0.2304	0.3259	0.3559	1.90e-12	0.1070	0.0027

Based on the method presented above, the flowchart of the proposed method for SOC estimation is shown in Fig. 2.

IV. EXPERIMENTS AND RESULTS DISCUSSION

In this study, 18,650 LiNiMnCoO₂/Graphite (LiNMC) lithium-ion cells are utilized for experimental verification. The whole testing process consists of an open circuit voltage OCV-SOC mapping test, dynamic stress test (DST) and federal urban driving schedule (FUDS) test. Before the DST and FUDS tests, the cells are charged with constant current and constant voltage (CCCV) with a standard current protocol and discharged to SoC=80% with 0.5C after complete equalization. The experimental temperature is fixed at room temperature (25 °C), and the effect of the change in battery capacity on the experimental results in a single cycle is disregarded. Basic information of the cell is shown in Table 1.

During the OCV-SOC mapping test, the low current (C/20) is utilized in the charge and discharge cycles and the measured terminal voltage is approximated as open circuit voltage with small current (C/20) excitation. The OCV test results are shown in Fig. 3. The nonlinear least-squares (LS) method is applied to identify the parameters of the OCV-SOC function, which is described by (2). The results are provided in Table 2. The root means square error (RMSE) of the parameter identification is 0.0098, which indicates that the formula in (2) can accurately track the relationship between OCV and SOC.

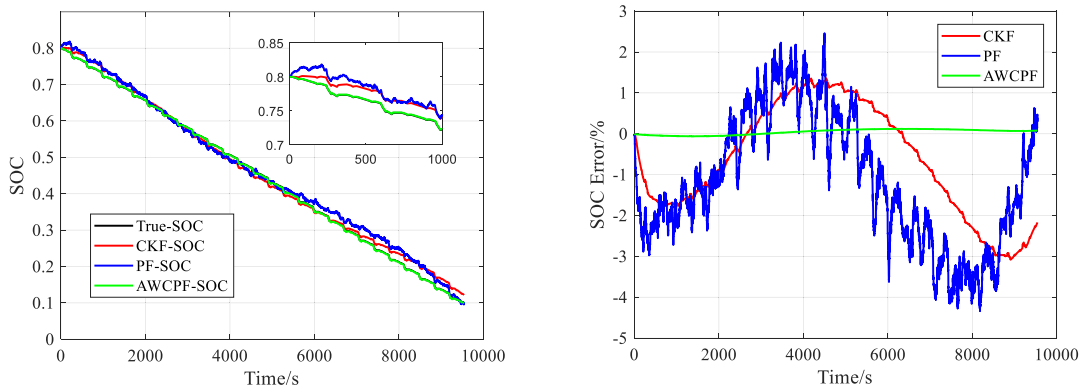


FIGURE 5. SOC estimation results under DST test condition by three methods.

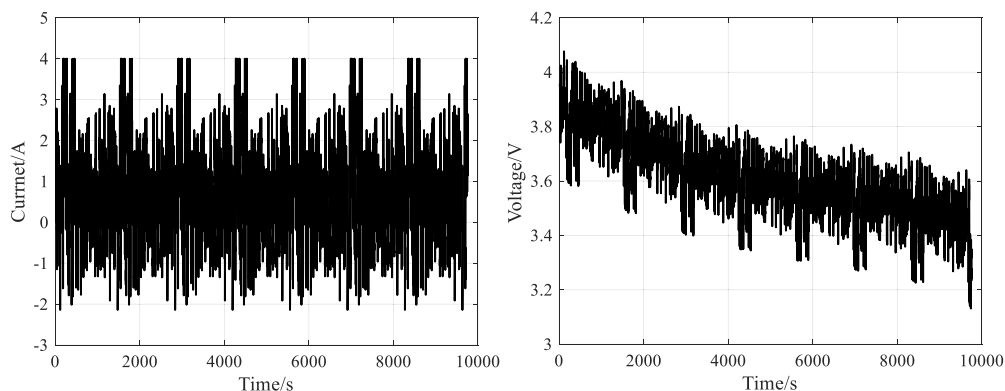


FIGURE 6. The current and voltage profiles under FUDS test condition.

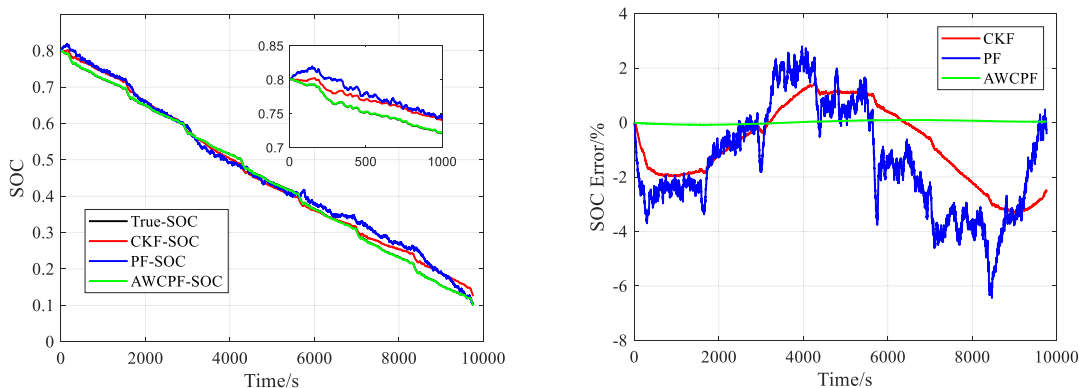


FIGURE 7. SOC estimation results under FUDS test condition by three methods.

The voltage and current data are measured by the NEWARE BTS battery test system for SOC estimation and algorithm verification. For comparison, the PF and CKF algorithms are also applied for SOC estimation.

The particle size of the AWCPF and PF methods is set to 50. The initial SOC value is set to the accurate value 0.8 to verify the accuracy of SOC estimation. The current and voltage profiles of the DST and FUDS tests are shown in Fig. 4 and Fig. 6.

As shown in Fig. 5, in the DST test condition, the proposed method AWCPF can accurately estimate the SOC with a small estimation error, while the estimation error of the CKF and PF are larger and the PF algorithm exhibits more fluctuations which may be caused by the randomness of particle distribution and the resampling period. The DST test is a simple and predictable cycle condition, while the FUDS test is a more complicated and fluctuated condition, as shown in Fig. 6, which may be more challenging for SOC

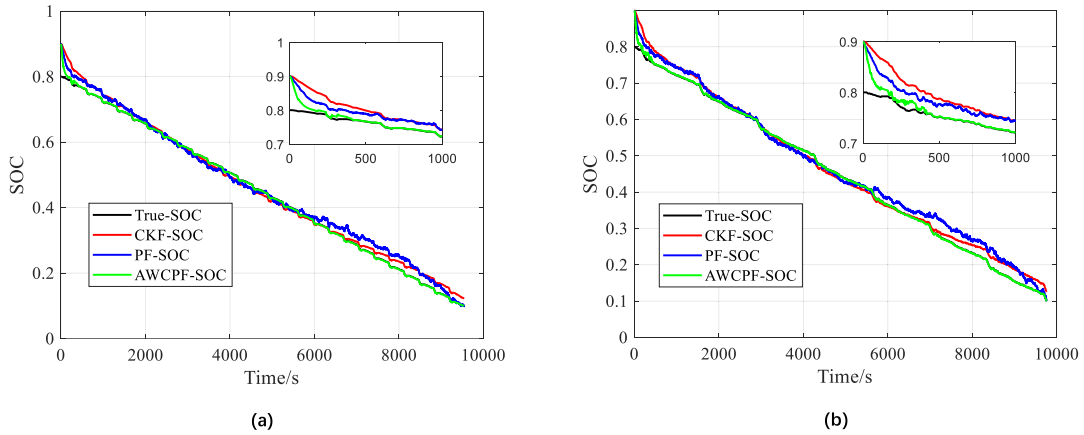


FIGURE 8. SOC estimation results with incorrect initial SOC value 0.9: (a) DST; (b) FUDS.

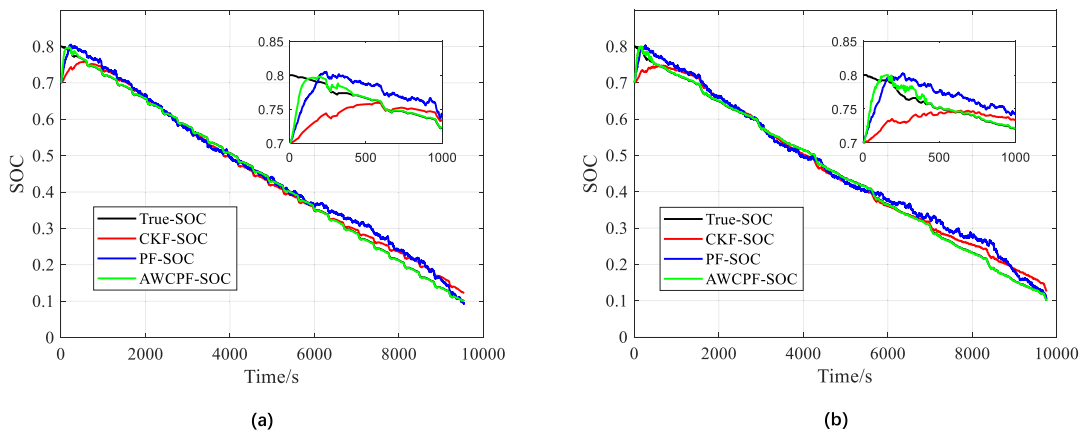


FIGURE 9. SOC estimation results with incorrect initial SOC value 0.7: (a) DST; (b) FUDS.

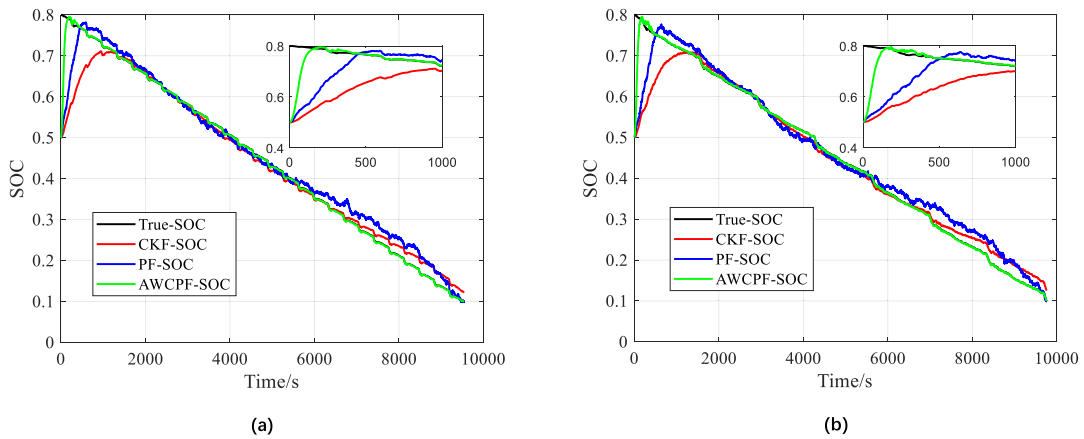


FIGURE 10. SOC estimation results with incorrect initial SOC value 0.5: (a) DST; (b) FUDS.

estimation. The SOC estimation results in the FUDS test condition are shown in Fig. 7. The proposed method can obtain accurate SOC estimation, while the SOC estimation error of the CKF and PF increased, which demonstrates the excellent adaptivity of the proposed method for complicated conditions.

To validate the convergence and robustness of the developed method, the initial value of the SOC is set to an incorrect value of 0.9, 0.7, and 0.5. The SOC estimation results with an incorrect initial SOC value are shown in Fig. 8-10. The results indicate that the proposed algorithm can converge to the true SOC value in a short time and is faster and more

TABLE 3. Performance of algorithms.

Algorithms	SOC estimation	Single iteration	Convergence
	RMSE	time /s	time /s
CKF	0.0521	0.0068	1195
PF	0.0427	0.0571	450
AWCPF	0.0205	0.0597	199

stable than the CKF and PF with a slight deviation in the initial SOC value by a ± 0.1 offset. For a large deviation, the initial SOC value is 0.5, and the proposed AWCPF method can rapidly converge to true value and exhibit a performance that is superior to CKF and PF.

To evaluate the computational efficiency of the proposed algorithm, a simulation was conducted on a laptop equipped with an Intel Core i7-7700 HQ processor (6 MB cache, up to 3.5 GHz) using MATLAB R2017a software. The comparison results with the PF and CKF algorithms are listed in Table 3. The SOC estimation RMSE is the root mean square error of the SOC estimation with an incorrect initial SOC value of 0.5 in the DST cycle condition. The Single iteration time denotes the time of one-step state estimation when single measured data are available, which is sampled by 1 Hz. The Convergence time represents the time of the estimation of the SOC converging to the real SOC value with an incorrect initial SOC value of 0.5 in the DST cycle condition, as shown in Fig. 10. As shown in the table, the proposed algorithm AWCPF has superior performance at the cost of higher computation compared with the CKF algorithm. However, if the initial value of SOC is offset, such as to 0.5, the AWCPF algorithm can rapidly converge to the real value with the minimum convergence time. Compared with the PF algorithm, the AWCPF can converge to the real value two times faster with only a small increase in the Single iteration time.

V. CONCLUSION

This paper proposed a novel SOC estimation method that is based on a particle filter algorithm. The dynamic characteristic of the battery is described by the first-order RC equivalent circuit model and the model parameters of the model are identified by a heuristic nature inspired improved ant lion optimization (IALO) algorithm. The SOC of the battery is estimated by the PF algorithm. To overcome the particle impoverishment shortage that exists in the PF algorithm, the Cubature Kalman filter algorithm has been used to generate the approximate optimum proposal distribution for the PF algorithm by integrating the last state estimation and latest measurement information. The system noise, prediction state measurement vector and covariance of the CKF are adaptively estimated. To restrain the influence of system noise to state estimation, the weights of the cubature points, which are generally constant, are adaptively adjusted based on the residual vector of state and measurement.

The proposed SOC estimation method AWCPF is tested and verified by experimental results. The results show that the AWCPF algorithm can obtain superior SOC estimation with

a small estimation error. The high performance robustness of the proposed method has been verified by estimating the SOC with high accuracy in the large initial SOC value deviation. With the rapid development of machine learning and data mining technology, the machine learning based SOC estimation methods will be investigated in subsequent research.

REFERENCES

- [1] M. A. Roscher and D. U. Sauer, "Dynamic electric behavior and open-circuit-voltage modeling of LiFePO₄-based lithium ion secondary batteries," *J. Power Sources*, vol. 196, pp. 331–336, Jan. 2011.
- [2] Y. Xing, E. W. M. Ma, K. L. Tsui, and M. Pecht, "Battery management systems in electric and hybrid vehicles," *Energies*, vol. 4, no. 11, pp. 1840–1857, 2011.
- [3] X. Zhang, Y. Wang, D. Yang, and Z. Chen, "An on-line estimation of battery pack parameters and state-of-charge using dual filters based on pack model," *Energy*, vol. 115, pp. 219–229, Nov. 2016.
- [4] F. Sun and R. Xiong, "A novel dual-scale cell state-of-charge estimation approach for series-connected battery pack used in electric vehicles," *J. Power Sour.*, vol. 274, pp. 582–594, Jan. 2015.
- [5] H. Dai, X. Wei, Z. Sun, J. Wang, and W. Gu, "Online cell SOC estimation of Li-ion battery packs using a dual time-scale Kalman filtering for EV applications," *Appl. Energy*, vol. 95, pp. 227–237, Jul. 2012.
- [6] X. Zhao, S. Wang, and M. Yu, "The comparison of soc estimation performance with different input parameters using neural network," *J. Mech. Eng. R&D*, vol. 1, pp. 730–735, Sep. 2016.
- [7] L. Lu, X. Han, J. Li, J. Hua, and M. Ouyang, "A review on the key issues for lithium-ion battery management in electric vehicles," *J. Power Sour.*, vol. 226, pp. 272–288, Mar. 2013.
- [8] H. Ren, Y. Zhao, S. Chen, and T. Wang, "Design and implementation of a battery management system with active charge balance based on the SOC and SOH online estimation," *Energy*, vol. 166, pp. 908–917, Jan. 2019.
- [9] X. Liu, J. Ma, X. Zhao, Y. Zhang, K. Zhang, and Y. He, "Integrated component optimization and energy management for plug-in hybrid electric buses," *Processes*, vol. 7, p. 477, Aug. 2019.
- [10] R. Xiong, H. He, F. Sun, and K. Zhao, "Evaluation on state of charge estimation of batteries with adaptive extended Kalman filter by experiment approach," *IEEE Trans. Veh. Technol.*, vol. 62, no. 1, pp. 108–117, Jan. 2013.
- [11] H. He, X. Zhang, R. Xiong, Y. Xu, and H. Guo, "Online model-based estimation of state-of-charge and open-circuit voltage of lithium-ion batteries in electric vehicles," *Energy*, vol. 39, no. 1, pp. 310–318, Mar. 2012.
- [12] F. Zheng, Y. Xing, J. Jiang, B. Sun, J. Kim, and M. Pecht, "Influence of different open circuit voltage tests on state of charge online estimation for lithium-ion batteries," *Appl. Energy*, vol. 183, pp. 513–525, Dec. 2016.
- [13] X. Zhao, S. Wang, J. Ma, Q. Yu, Q. Gao, and M. Yu, "Identification of driver's braking intention based on a hybrid model of GHMM and GGAP-RBFNN," *Neural Comput. Appl.*, vol. 31, no. 1, pp. 161–174, Jan. 2019.
- [14] L. Kang, X. Zhao, and J. Ma, "A new neural network model for the state-of-charge estimation in the battery degradation process," *Appl. Energy*, vol. 121, pp. 20–27, May 2014.
- [15] X. Zhao, Q. Yu, J. Ma, Y. Wu, M. Yu, and Y. Ye, "Development of a representative EV urban driving cycle based on a K-means and SVM hybrid clustering algorithm," *J. Adv. Transp.*, vol. 2018, Nov. 2018, Art. no. 1890753.
- [16] X. Zhao, S. Xu, Y. Ye, M. Yu, and G. Wang, "Composite braking AMT shift strategy for extended-range heavy commercial electric vehicle based on LHMM/ANFIS braking intention identification," *Cluster Comput.*, vol. 1, pp. 1–16, Feb. 2018.
- [17] J. Han, D. Kim, and M. Sunwoo, "State-of-charge estimation of lead-acid batteries using an adaptive extended Kalman filter," *J. Power Sources*, vol. 188, no. 2, pp. 606–612, Mar. 2009.
- [18] Z. Chen, S. Qiu, M. A. Masrur, and Y. L. Murphey, "Battery state of charge estimation based on a combined model of extended Kalman Filter and neural networks," in *Proc. Int. Joint Conf. Neural Netw.*, Jul./Aug. 2011, pp. 2156–2163.
- [19] G. L. Plett, "Extended Kalman filtering for battery management systems of LiPB-based HEV battery packs: Part 2. Modeling and identification," *J. Power Sour.*, vol. 134, no. 2, pp. 262–276, 2004.

- [20] D. Wang, Y. Bao, and J. Shi, "Online lithium-ion battery internal resistance measurement application in state-of-charge estimation using the extended kalman filter," *Energies*, vol. 10, p. 1284, Aug. 2017.
- [21] W. He, N. Williard, C. Chen, and M. Pecht, "State of charge estimation for Li-ion batteries using neural network modeling and unscented Kalman filter-based error cancellation," *Int. J. Elect. Power Energy Syst.*, vol. 62, pp. 783–791, Nov. 2014.
- [22] Q. Yu, R. Xiong, and C. Lin, "Online estimation of state-of-charge based on the H infinity and unscented Kalman filters for lithium ion batteries," *Energy Proc.*, vol. 105, pp. 2791–2796, May 2017.
- [23] M. Partovibakhsh and G. Liu, "An adaptive unscented Kalman filtering approach for online estimation of model parameters and state-of-charge of lithium-ion batteries for autonomous mobile robots," *IEEE Trans. Control Syst. Technol.*, vol. 23, no. 1, pp. 357–363, Jan. 2015.
- [24] Y. Li, C. Wang, and J. Gong, "A wavelet transform-adaptive unscented Kalman filter approach for state of charge estimation of LiFePO₄ battery," *Int. J. Energy Res.*, vol. 42, pp. 587–600, Feb. 2018.
- [25] K. Zhang, J. Ma, X. Zhao, X. Liu, and Y. Zhang, "Parameter identification and state of charge estimation of NMC cells based on improved ant lion optimizer," *Math. Problems Eng.*, vol. 2019, Jul. 2019, Art. no. 4961045.
- [26] N. J. Gordon, D. J. Salmond, and A. F. M. Smith, "Novel approach to nonlinear/non-Gaussian Bayesian state estimation," *IEE Proc. F Radar Signal Process.*, vol. 140, pp. 107–113, Apr. 1993.
- [27] A. Tulsyan, Y. Tsai, R. B. Gopaluni, and R. D. Braatz, "State-of-charge estimation in lithium-ion batteries: A particle filter approach," *J. Power Sources*, vol. 331, pp. 208–223 Nov. 2016.
- [28] M. Ye, H. Guo, R. Xiong, and Q. Yu, "A double-scale and adaptive particle filter-based online parameter and state of charge estimation method for lithium-ion batteries," *Energy*, vol. 144, pp. 789–799, Feb. 2018.
- [29] D. Jiani, W. Youyi, and W. Changyun, "Li-ion battery SOC estimation using particle filter based on an equivalent circuit model," in *Proc. 10th IEEE Int. Conf. Control Automat. (ICCA)*, Jun. 2013, pp. 580–585.
- [30] Z. Chen, H. Sun, G. Dong, J. Wei, and J. Wu, "Particle filter-based state-of-charge estimation and remaining-dischargeable-time prediction method for lithium-ion batteries," *J. Power Sources*, vol. 414, pp. 158–166, Feb. 2019.
- [31] T. Zahid, G. Xu, W. Li, L. Zhao, and K. Xu, "Performance analysis of particle filter for SOC estimation of LiFePO₄ battery pack for electric vehicles," in *Proc. IEEE Int. Conf. Inf. Automat. (ICIA)*, Hailar, China, Jul. 2014, pp. 1061–1065.
- [32] S. Li, L. Li, Z. Li, X. Chen, T. Fernando, H. H.-C. Iu, G. He, "Event-trigger heterogeneous nonlinear filter for wide-area measurement systems in power grid," *IEEE Trans. Smart Grid*, vol. 10, no. 3, pp. 2752–2764, May 2019.
- [33] Y. Yu, Z. Li, X. Liu, K. Hirota, X. Chen, T. Fernando, and H. H.-C. Iu, "A nested tensor product model transformation," *IEEE Trans. Fuzzy Syst.*, vol. 27, no. 1, pp. 1–15, Jan. 2019.
- [34] X. Liu, L. Li, Z. Li, X. Chen, T. Fernando, H. H.-C. Iu, and G. He, "Event-trigger particle filter for smart grids with limited communication bandwidth infrastructure," *IEEE Trans. Smart Grid*, vol. 9, no. 6, pp. 6918–6928, Nov. 2018.
- [35] B. Liu, Z. Li, X. Chen, Y. Huang, and X. Liu, "Recognition and vulnerability analysis of key nodes in power grid based on complex network centrality," *IEEE Trans. Circuits Syst. II, Exp. Briefs*, vol. 65, no. 3, pp. 346–350, Mar. 2018.
- [36] S. Li, Y. Hu, L. Zheng, X. Chen, T. Fernando, H. C. Lu, Q. Wang, and X. Liu, "Stochastic event-triggered cubature Kalman filter for power system dynamic state estimation," *IEEE Trans. Circuits Syst. II, Exp. Briefs*, vol. 66, no. 9, pp. 1552–1556, Sep. 2019.
- [37] X. Liu, L. Li, Z. Li, T. Fernando, and H. H. C. Iu, "Stochastic stability condition for the extended Kalman filter with intermittent observations," *IEEE Trans. Circuits Syst. II, Exp. Briefs*, vol. 64, no. 3, pp. 334–338, Mar. 2017.
- [38] Y. He, X. Liu, C. Zhang, and Z. Chen, "A new model for State-of-Charge (SOC) estimation for high-power Li-ion batteries," *Appl. Energy*, vol. 101, pp. 808–814, Jan. 2013.
- [39] Y. Shen, "Hybrid unscented particle filter based state-of-charge determination for lead-acid batteries," *Energy*, vol. 74, pp. 795–803, Sep. 2014.
- [40] I. Arasaratnam, S. Haykin, and T. R. Hurd, "Cubature Kalman filtering for continuous-discrete systems: Theory and simulations," *IEEE Trans. Signal Process.*, vol. 58, no. 10, pp. 4977–4993, Oct. 2010.
- [41] B. Xia, H. Wang, M. Wang, W. Sun, Z. Xu, and Y. Lai, "A new method for state of charge estimation of lithium-ion battery based on strong tracking cubature Kalman filter," *Energies*, vol. 8, pp. 13458–13472, Dec. 2015.
- [42] D. Wang, F. Yang, K.-L. Tsui, Q. Zhou, and S. J. Bae, "Remaining useful life prediction of lithium-ion batteries based on spherical cubature particle filter," *IEEE Trans. Instrum. Meas.*, vol. 65, no. 6, pp. 1282–1291, Jun. 2016.
- [43] X. Lai, Y. Zheng, and T. Sun, "A comparative study of different equivalent circuit models for estimating state-of-charge of lithium-ion batteries," *Electrochim. Acta*, vol. 259, pp. 566–577, Jan. 2018.
- [44] S. Peng, X. Zhu, Y. Xing, H. Shi, X. Cai, and M. Pecht, "An adaptive state of charge estimation approach for lithium-ion series-connected battery system," *J. Power Sources*, vol. 392, pp. 48–59, Jul. 2018.
- [45] B. Xia, H. Wang, Y. Tian, M. Wang, W. Sun, and Z. Xu, "State of charge estimation of lithium-ion batteries using an adaptive cubature Kalman filter," *Energies*, vol. 8, pp. 5916–5936, Jun. 2015.



KAI ZHANG received the B.S. degree in vehicle engineering from Chang'an University, Xi'an, China, in 2013, where he is currently pursuing the Ph.D. degree in automobile engineering. His research interests include electric vehicle control strategy and power battery state estimation.



JIAN MA received the Ph.D. degree in transportation engineering from Chang'an University, China, in 2001. He is currently a Professor with the School of Automobile Engineering, Chang'an University. He has undertaken more than 30 government-sponsored research projects, such as 863 projects and key transportation projects in China. He has published more than 90 academic articles at home and abroad. He has authored four books. His main research interests include vehicle dynamics, electric vehicle and clean energy vehicle technology, and automobile detection technology and theory.



XUAN ZHAO received the B.S., M.S., and Ph.D. degrees in vehicle engineering from Chang'an University, China, in 2007, 2009, and 2012, respectively, where he is currently an Associate Professor with the School of Automobile Engineering. He has undertaken over nine government sponsored works, including the National Key Research and Development Program of China and the China Postdoctoral Science Foundation. His main research interests include electric vehicle control strategy and electric vehicle lightweight design.



DAYU ZHANG received the B.S. degree in vehicle engineering from Chang'an University, China, in 2017, where he is currently pursuing the M.S. degree in automobile engineering. His main research interests include power battery management and energy system optimization.



YILIN HE received the B.S., M.S., and Ph.D. degrees in vehicle engineering from Chang'an University, China, in 2011, 2014, and 2018, respectively. She is currently an Engineer with the School of Automobile Engineering, Chang'an University. She has undertaken four works sponsored by Chang'an University. Her main research interest includes intelligent electric vehicle control strategy.

• • •